The Electro-Oxidation of Hydrazine: A Self-Inhibiting Reaction

Ruiyang Miao, Richard G Compton*

Department of Chemistry, Physical and Theoretical Chemistry Laboratory, University of Oxford, South Parks Road, Oxford OX1 3QZ, England

*Corresponding author

Email: richard.compton@chem.ox.ac.uk

Phone: +44 (0) 1865 275957 Fax: +44 (0) 1865 275410

Abstract

The electro-oxidation of hydrazine to form di-nitrogen is reported over a wide range of both pH and of unbuffered conditions at glassy carbon electrodes. It is shown that hydrazine molecules are only electro-active in their un-protonated form, N_2H_4, whereas the protonated species $N_2H_5^+$ is electro-inactive. The oxidation of N_2H_4 releases four protons per molecule which are diffusing away from the electrode rapidly (on the voltammetric timescale) protonate unreacted N_2H_4 molecules diffusing to the electrode converting them into the electro-inactive form, $N_2H_5^+$; the reaction is *self-inhibiting* and the currents flowing are significantly reduced compared to those expected for a simple electrolytic conversion to an extent reflecting the pH and buffer content of the solution local to the electrode. The local pH in turn is controlled partly by the quantity of protons released electrolytically. The self-inhibition is modelled by solving the relevant transport equations with coupled homogeneous chemical kinetics, utilising Marcus-Hush electron transfer, giving predicted reduced currents reflecting the pK_a and kinetics of the $N_2H_4/N_2H_5^+$ equilibrium in excellent agreement with experimental voltammetric waveshapes.

Keywords: hydrazine; electrode kinetics; oxidative proton release; self-inhibition; Marcus-Hush theory

TOC Graphic

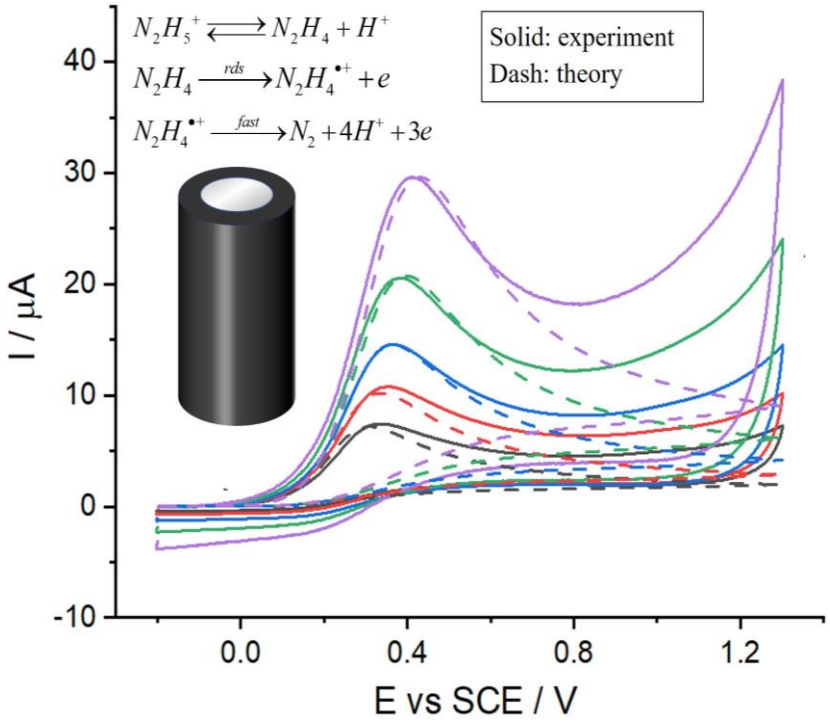

The oxidation of hydrazine at the glassy carbon surface is self-inhibited that the protons released from the oxidation combine with the hydrazine diffusing towards the surface to form the inactive protonated hydrazine.

The fundamental electrochemistry of hydrazine is fascinating since it presents two challenges. The first of these relates to the unusual voltammetry seen, even in carbon electrodes,[1] in which the voltammetric waves increase only gradually with potential in contrast to the predictions of the semi-empirical Butler-Volmer theory[2-3] widely used to interpret electrode kinetic data.[4] Note that there is either zero or only very weak adsorption of hydrazine molecules at carbon surfaces.[5] The second relates to the magnitude of the currents flowing which, at first sight, suggest either the passage of less than four electrons per molecule of hydrazine or that the latter has a pathologically low diffusion coefficient in aqueous solution. Indeed a review of the literature of the electrochemically determined diffusion coefficients of hydrazine showed values ranging for different media implausibly over a factor of ca. 35 with many values much lower than expected for a molecule of the size of hydrazine.[6-11]

In a recent paper the first of these challenges, namely the voltammetric wave shape, was addressed[1] under conditions where N_2H_4 is the sole solution phase species and the effect shown to originate in a potential dependent transfer coefficient which in turn was shown to result from the operation of Marcus-Hush (as opposed to Butler-Volmer) electron transfer kinetics[12-13] with a rather low re-organisation energy and controlling the first electron transfer and which was seen to be rate determining, at least at carbon electrodes.

In the present paper we address the second and greater challenge noting that the oxidation of hydrazine produces protons which on account of the basicity of the molecule may protonate N_2H_4 forming $N_2H_5^+$ in aqueous solution. Thus we hypothesise

that the protons released in the electro-oxidation can interfere with the electrode reaction by altering the chemical speciation adjacent to the electrode by altering the local solution pH. Specifically we suggest that the local formation of increased quantities of acid and hence of the $N_2H_5^+$ cation changes the voltammetric response because of the contrasting electrochemical activity of the cation in comparison with the precursor N_2H_4. In particular, on the basis of the voltammetry over a range of pH values and buffer compositions, the former is shown not to be electroactive at carbon electrodes in contrast to the latter. Detailed modelling, based on Marcusian electron transfer kinetics, and the homogeneous chemistry of the $N_2H_4/N_2H_5^+$ acid-base equilibrium, both thermodynamic and kinetic, are shown to validate this hypothesis. The experimental details are provided in the Supporting Information (SI) Section 1.

In the following we consider the voltammetry of hydrazine in aqueous solutions of different pH. It is helpful therefore to consider first the speciation of hydrazine noting the pK_{a1} value of ca. 8.0[14-17] and the pK_{a2} of ca. -1.0[18-20] at 298 K which correspond to the following chemical equilibria

$$N_2H_5^+ \rightleftharpoons N_2H_4 + H^+ \quad (1)$$

$$N_2H_6^{2+} \rightleftharpoons N_2H_5^+ + H^+ \quad (2)$$

The speciation of hydrazine as a function of pH in pure water is shown in the SI Section 2, Figure S1. In practice the exact speciation at any pH may likely also reflect to some small extent the total electrolyte concentration in the solution, the so-called salt effect;[21-22] this is considered further below.

The oxidation of hydrazine was first studied electrochemically at a glassy carbon

electrode (GCE) in solutions of 1.5 mM hydrazine supported by 0.1 M KNO_3 which had been adjusted to pH 2.0 or pH 7.0 by the addition of tiny amounts of 1 M HNO_3. Note that the dominant species in the solution of pH 2.0 is almost 100% hydrazinium cation $N_2H_5^+$ as shown in Figure S1. As depicted in Figure 1A (pH 2.0), there are no additional oxidative features seen in the voltammogram (solid line) as compared to the also featureless control experiment conducted in the absence of hydrazine (dash line). This clearly shows that there is no direct oxidation of $N_2H_5^+$ on the surface of the GCE. In contrast, Figure 1B (pH 7.0) shows a fully electrochemically irreversible wave[23] with a peak at ca. 0.36 V vs SCE of a current of 2.0 μA (solid line); no voltammetric features were observed in the absence of hydrazine (dash line). It is deduced that the anodic current results from the oxidation of the unprotonated hydrazine N_2H_4 given the 'inactivity' of $N_2H_5^+$ and the negligible concentration of $N_2H_6^{2+}$ in solution (Figure S1).

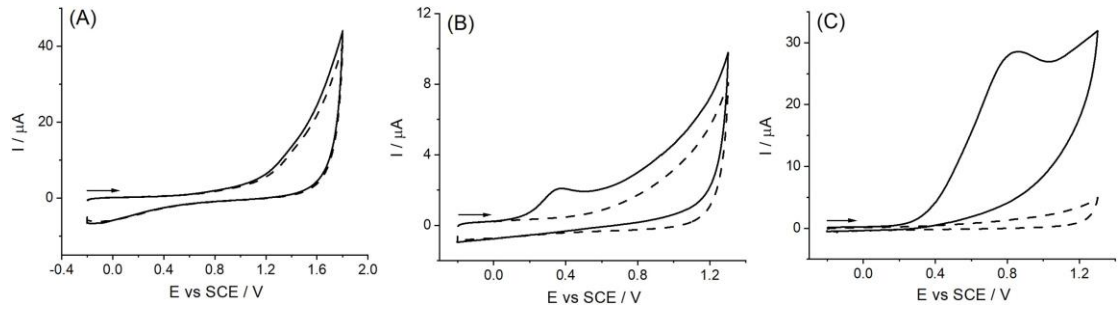

Figure 1. Cyclic voltammetry (solid line) at a GCE of 1.5 mM hydrazine supported by the electrolytes: (A) 0.1 M KNO_3, pH 2 (see text), (B) 0.1 M KNO_3 of pH 7 (see text) and (C) 0.1 M PBS of pH 7. The control experiments without hydrazine are shown as the dash lines in each case. Scan rate: 50 mV/s. The arrows indicate the start potential of the voltammetric scans and the direction of sweep. The voltammograms at different scan rates (25 - 400 mV/s) are provided in the Supporting Information (SI) Section 3.

It is widely recognized that the oxidation of N_2H_4 is a four-electron transfer process with the release of protons and forming nitrogen N_2.[24-26] The expulsion of protons necessarily changes the local pH (of the solution close to the surface of the GCE). To

investigate the effect of the local pH variation on the reaction process, 1.5 mM hydrazine supported by phosphate buffer solution (PBS) with a total concentration of 0.1 M was utilized as the electrolyte for comparison and contrast. The voltammograms were recorded and are presented in Figure 1C where a clear oxidative peak is observed at ca. 0.85 V vs SCE with a current of ca. 28 μA. Note that there is a dramatic increase in peak current compared to that in Figure 1B, when, as in Figure 1C, the local proton concentration is largely fixed by the buffer which can combine with the protons released from the electrolysis. The observed potential shift is likely ascribed to the change in the local composition and hence of mass transport of the analyte as the buffer system is introduced. It is inferred that in the KNO_3 electrolyte, the protons released from the oxidation of N_2H_4 and diffusing away from the electrode likely combine with the incoming N_2H_4 molecules diffusing to the electrode to form the 'inactive' $N_2H_5^+$ that, as shown above, is not oxidised at the GCE. This gives rise to the very small anodic current seen in the unbuffered solution (Figure 1B) resulting from the N_2H_4 which does not become protonated as it diffuses to the electrode. In other words, the process of hydrazine oxidation on the surface of the GCE is limited to a great extent by the synchronous *self-inhibition* effect from the combination of N_2H_4 molecules and oxidation-produced H^+. This finding is of great significance to all practical uses employing the electro-oxidation of hydrazine, for example and especially in amperometric sensors for this toxic material[27-28] as well as the correct quantitative interpretation of hydrazine electrochemistry at all electrodes of any chemical composition.

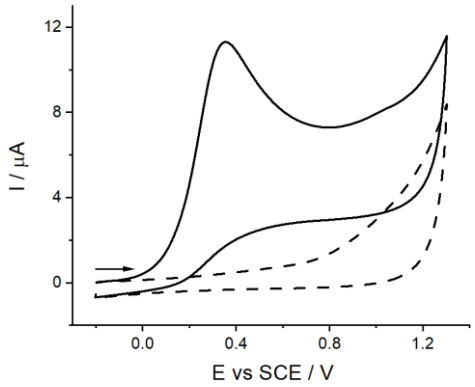

Figure 2. Cyclic voltammetry (solid line) at a GCE of 1.5 mM hydrazine supported by 0.1 M KNO_3 of pH 9.7. The control experiment without hydrazine is presented as the dash line. Scan rate: 50 mV/s. The arrow indicates the start potential and direction of the voltammetric scan. The voltammograms at different scan rates (25 - 400 mV/s) are provided in the SI Section 4.

To probe into the *intrinsic* electron transfer of hydrazine oxidation and the homogeneous dynamics between the redox active N_2H_4 and the redox inactive $N_2H_5^+$, cyclic voltammetry was conducted at a GCE in a system where 1.5 mM hydrazine was solely supported by 0.1 M KNO_3, *without* the addition of any mineral acid or of buffer solution. The pH was determined to be 9.7 as mentioned above. This value implies a pK_a value of 8.3 which compares with the reported value of ~8.0 for pure water at the same temperature (298K)[14-17] implying a small thermodynamic salt effect due to the dissolved KNO_3. The recorded anodic current, as displayed in Figure 2, is distinctly larger than that seen for (the acid adjusted) pH 7.0 (0.1 M KNO_3) in Figure 1B. The increase mainly results from the enhanced concentration of the electro-active N_2H_4 in bulk solution as seen in Figure S1. The current is however less than that expected for a simple diffusion-controlled oxidation of hydrazine reflecting the self-inhibition effect noted above.

DIGISIM is a well-respected commercial simulation software (BASI, West Lafayette, USA) for cyclic voltammetry based on the fast implicit finite difference method

invented by M Rudolph.[29-30] This was utilized to facilitate the analysis of the hydrazine electro-oxidation reaction mechanism and to quantify the associated kinetics on the voltammetric waveshape, the peak currents and the inferred potential dependent transfer coefficient. A planar geometry was adopted in the simulation corresponding to the experimentally deployed macrodisc GCE of 3.0 mm in diameter under a transport regime dominated by linear diffusion.[31] The first electron transfer of the N_2H_4 oxidation process at pH 2 - 11 was found in our recent work[32] to be rate-determining via the nanoimpact technique. This rate determining step (rds) involves no release of protons, which are expelled in subsequent steps. Thus the rds was inferred in the case of carbon electrodes to involve the formation of the transient radical cation $N_2H_4^{\bullet+}$ on the surface of the electrode or in the solution. The hydrazinium cation $N_2H_5^+$ is not oxidised as mentioned above. Hence, the mechanism was proposed as follows:

$$N_2H_5^+ \rightleftarrows N_2H_4 + H^+$$

$$N_2H_4 \xrightarrow{rds} N_2H_4^{\bullet+} + e$$

$$N_2H_4^{\bullet+} \xrightarrow{fast} N_2 + 4H^+ + 3e$$

where the equilibrium constant for the homogeneous chemical reaction was adopted from the experimentally determined pK_a value for 0.1 M KNO_3 aqueous solution as mentioned above and the homogeneous second order rate constant (M^{-1} s^{-1}) for reaction of protons with hydrazine was optimised to give the best fit between experiment and simulation. Independently measured[32] diffusion coefficients for N_2H_4 and $N_2H_5^+$ were used together with a literature value for the proton diffusion coefficient.[33-34] Note that fixing the K_a value and the second order rate constant necessarily defines the first order

rate constant for the dissociation of the hydrazinium cation. The electron transfer kinetics were assumed to be governed by Marcus-Hush theory in the light of the data presented in the SI Section 5 and our previous work[1] which demonstrated that the Marcus-Hush theory[12-13] was required to describe the hydrazine oxidation, instead of the potential independent transfer coefficient as assumed in the phenomenological Butler-Volmer kinetics[2-3, 35]. The reorganization energy in the more physically based Marcus-Hush formalism reflects both solvent polarisation and internal molecular vibration. Accordingly the Marcusian kinetics was selected as the mathematical model in DIGISIM and the previously measured value of 0.35 eV used as the reorganisation energy. The details of the simulation are provided in the SI Section 6.

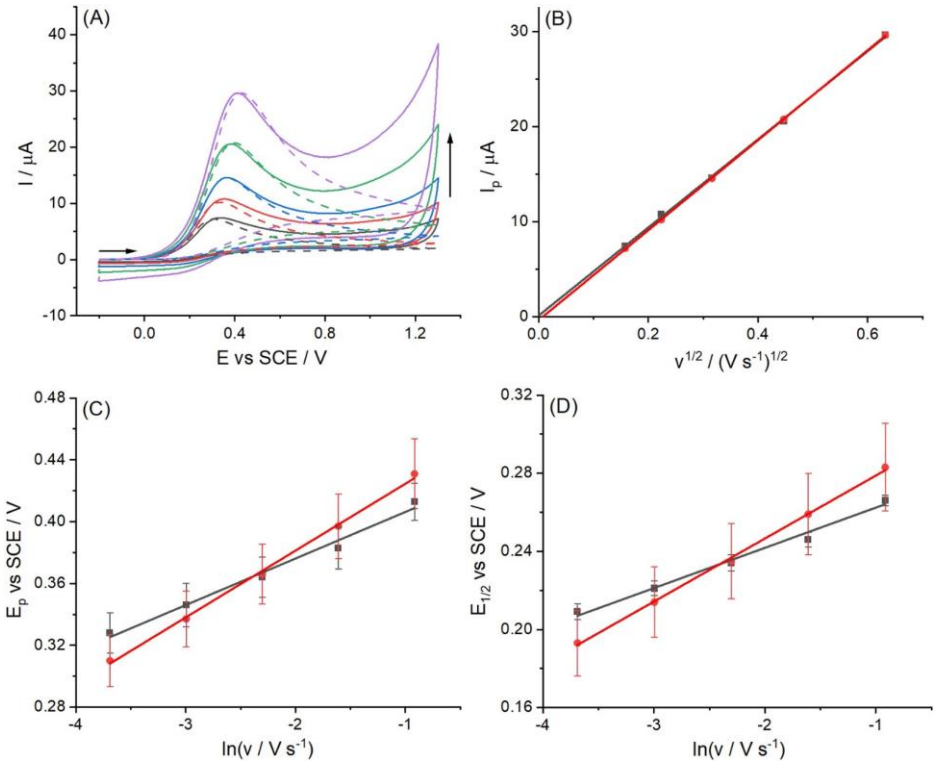

Figure 3. The comparison between the experimental and DIGISIM-simulated voltammetry at a GCE of 1.5 mM hydrazine supported by 0.1 M KNO_3 of pH 9.7: (A) the voltammograms (solid for experiment, dash for simulation); (B) the plot of I_p versus $v^{1/2}$; (C) the plot of E_p versus ln$v$ and (D) $E_{1/2}$ versus ln$v$ (black for experiment, red for simulation). Note that the experimental voltammograms are baseline-corrected. The transverse arrow indicates the start potential and

direction of the voltammetric scan. The vertical arrow indicates increasing scan rates. Simulation parameters: initial concentrations of N_2H_4, $N_2H_5^+$ and H^+ are 1.44 mM, 0.06 mM and 2×10^{-10} M respectively; formal potential of $N_2H_4/N_2H_4^{\bullet+}$ is 0.14 V; reorganization energy is 0.35 eV; equilibrium constant of $N_2H_4/N_2H_5^+$ is 5.0×10^{-9} M; diffusion coefficients of N_2H_4 and $N_2H_5^+$ are 7.1×10^{-6} cm^2/s and 2.8×10^{-6} cm^2/s respectively; standard rate constant of the rds step is 4.5×10^{-5} cm/s; second order rate constant for the protonation of hydrazine is 1.1×10^5 M^{-1} s^{-1}; scan rates are 25/50/100/200/400 mV/s.

Figure 3A shows the favourable comparison between the experimental voltammograms and the simulated predictions of the above model (using exactly the same parameters) at scan rates in the range of 25 - 400 mV/s. A satisfactory fitting for the studied oxidative peak in terms of shape, size and position is observed for each scan rate. In particular the simulation captures the unusual 'drawn out' shape of the voltammetry which arises from the decrease of the transfer coefficient with potential; simulation using Butler-Volmer kinetics was unable to reproduce this feature. Note that the 'drawn out' shape (indicated in Figure S3) is distinguished from the typical electrochemically highly irreversible processes which display a much higher rate of increase of the current with potential.[1] Numerical information about current and potential are presented in the plots of I_p against $v^{1/2}$ (Figure 3B) as well as E_p (Figure 3C) and $E_{1/2}$ (Figure 3D) against ln*v*. Overall good consistency between experiment and theory is attained as is evident from the totality of the data presented in Figure 3. Finally the simulations allow the inference of a value of 0.14 V vs SCE for the standard electrode potential where this relates to the first and rate determining electron transfer

$$N_2H_4 \xrightarrow{rds} N_2H_4^{\bullet+} + e$$

This in turn allows an *approximate* estimation of the associated standard rate constant k_0 of $(4.5 \pm 1.0) \times 10^{-5}$ cm/s for the rate-determining step. Note that these numerical inferences presume the validity of the *symmetric* form of Marcus Hush theory and hence

are subject to that important caveat. The slow k_0 conforms to the full electrochemical irreversibility of hydrazine oxidation under the mass transport conditions prevailing.[36-37]

In conclusion, the oxidation of hydrazine in solutions of around neutral pH and more generally in unbuffered media is shown to be an intrinsically self-inhibiting reaction in which the protons released in the course of the oxidation combine with the reactant to form cations of protonated hydrazine which are not electroactive at carbon electrodes. The reaction has been modelled using Marcus-Hush theory which quantitatively and fully accounts for the observed voltammetry provided the thermodynamics and kinetics of the protonation are considered.

Notes

The authors declare no competing financial interest.

References

(1) Miao, R.; Chen, L.; Compton, R. G. Electro-oxidation of hydrazine shows Marcusian electron transfer kinetics. *Science China Chemistry* **2021,** *64*, 322-329.
(2) Erdey-Grúz, T.; Volmer, M. Zur frage der elektrolytischen metallüberspannung. *Z. Phys. Chem.* **1931,** *157* (1), 165-181.
(3) Butler, J. A. V. The mechanism of overvoltage and its relation to the combination of hydrogen atoms at metal electrodes. *Transactions of the Faraday Society* **1932,** *28*, 379-382.
(4) Batchelor-McAuley, C.; Kätelhön, E.; Barnes, E. O.; Compton, R. G.; Laborda, E.; Molina, A. Recent advances in voltammetry. *ChemistryOpen* **2015,** *4* (3), 224.
(5) Wang, B.; Cao, X. The anodic oxidation of hydrazine on glassy carbon electrode. *Electroanalysis* **1992,** *4* (7), 719-724.
(6) Daemi, S.; Ashkarran, A. A.; Bahari, A.; Ghasemi, S. Fabrication of a gold nanocage/graphene nanoscale platform for electrocatalytic detection of hydrazine. *Sensors and Actuators B: Chemical* **2017,** *245*, 55-65.
(7) Kaladevi, G.; Meenakshi, S.; Pandian, K.; Wilson, P. Synthesis of well-dispersed silver nanoparticles

on polypyrrole/reduced graphene oxide nanocomposite for simultaneous detection of toxic hydrazine and nitrite in water sources. *J. Electrochem. Soc.* **2017,** *164* (13), B620.
(8) Ali, S. M. Smart perovskite sensors: the electrocatalytic activity of $SrPdO_3$ for hydrazine oxidation. *J. Electrochem. Soc.* **2018,** *165* (9), B345.
(9) Zare, H. R.; Nasirizadeh, N. Hematoxylin multi-wall carbon nanotubes modified glassy carbon electrode for electrocatalytic oxidation of hydrazine. *Electrochim. Acta* **2007,** *52* (12), 4153-4160.
(10) Kamyabi, M.; Narimani, O.; Monfared, H. H. Electrocatalytic oxidation of hydrazine using glassy carbon electrode modified with carbon nanotube and terpyridine manganese (II) complex. *J. Electroanal. Chem.* **2010,** *644* (1), 67-73.
(11) Wang, L.; Meng, T.; Jia, H.; Feng, Y.; Gong, T.; Wang, H.; Zhang, Y. Electrochemical study of hydrazine oxidation by leaf-shaped copper oxide loaded on highly ordered mesoporous carbon composite. *J. Colloid Interface Sci.* **2019,** *549*, 98-104.
(12) Hush, N. Adiabatic rate processes at electrodes. I. Energy-charge relationships. *The Journal of Chemical Physics* **1958,** *28* (5), 962-972.
(13) Chidsey, C. E. Free energy and temperature dependence of electron transfer at the metal-electrolyte interface. *Science* **1991,** *251* (4996), 919-922.
(14) Grekov, A. Organic chemistry of hydrazine. *Tekhnika, Kiev* **1966**, 211-212.
(15) Meites, L. Handbook of analytical chemistry. *Soil Science* **1963,** *96* (5), 358.
(16) Rich, R. *Inorganic reactions in water*. Springer Science & Business Media: 2007.
(17) Krittayavathananon, A.; Srimuk, P.; Luanwuthi, S.; Sawangphruk, M. Palladium nanoparticles decorated on reduced graphene oxide rotating disk electrodes toward ultrasensitive hydrazine detection: effects of particle size and hydrodynamic diffusion. *Anal. Chem.* **2014,** *86* (24), 12272-12278.
(18) Zhakenovich, A. Y.; Valentina, Y.; Tussupbayev Nessipbay, S. T.; Zhadyra, Y. The Search for New Methods of Synthesis Possible of Organometallic Compounds of P, As, Sb, Bi. *J. Chem* **2015,** *9*, 500-502.
(19) Schirmann, J. P.; Bourdauducq, P. Hydrazine. *Ullmann's Encyclopedia of Industrial Chemistry* **2000**.
(20) Clearfield, A.; Karlin), K. Progress in inorganic chemistry. *John Wiley & Sons, Inc., New York* **1998,** *47*, 371-510.
(21) Debye, P.; Hückel, E. Zur theorie der elektrolyte. II. *Das Grenzgesetz für die elektrische Leitfähigkeit. Phys* **1923,** *305*.
(22) Malý, M.; Boublík, M.; Pocrnić, M.; Ansorge, M.; Lorinčíková, K.; Svobodová, J.; Hruška, V.; Dubský, P.; Gaš, B. Determination of thermodynamic acidity constants and limiting ionic mobilities of weak electrolytes by capillary electrophoresis using a new free software AnglerFish. *Electrophoresis* **2020,** *41* (7-8), 493-501.
(23) Compton, R. G.; Banks, C. E. *Understanding Voltammetry*. 3rd edition. World Scientific: 2018.
(24) Rees, N. V.; Compton, R. G. Carbon-free energy: a review of ammonia-and hydrazine-based electrochemical fuel cells. *Energy & Environmental Science* **2011,** *4* (4), 1255-1260.
(25) Lu, Z.; Sun, M.; Xu, T.; Li, Y.; Xu, W.; Chang, Z.; Ding, Y.; Sun, X.; Jiang, L. Superaerophobic electrodes for direct hydrazine fuel cells. *Adv. Mater.* **2015,** *27* (14), 2361-2366.
(26) de Oliveira, D. C.; Silva, W. O.; Chatenet, M.; Lima, F. H. NiO_x-Pt/C nanocomposites: highly active electrocatalysts for the electrochemical oxidation of hydrazine. *Applied Catalysis B: Environmental* **2017,** *201*, 22-28.
(27) Madhu, R.; Veeramani, V.; Chen, S.-M. Fabrication of a novel gold nanospheres/activated carbon nanocomposite for enhanced electrocatalytic activity toward the detection of toxic hydrazine in various

water samples. *Sensors and Actuators B: Chemical* **2014,** *204*, 382-387.
(28) Bansal, P.; Bhanjana, G.; Prabhakar, N.; Dhau, J. S.; Chaudhary, G. R. Electrochemical sensor based on ZrO_2 NPs/Au electrode sensing layer for monitoring hydrazine and catechol in real water samples. *J. Mol. Liq.* **2017,** *248*, 651-657.
(29) Rudolph, M. A fast implicit finite difference algorithm for the digital simulation of electrochemical processes. *Journal of electroanalytical chemistry and interfacial electrochemistry* **1991,** *314* (1-2), 13-22.
(30) Bott, A. Simulation of cyclic voltammetry using finite difference methods. *Current Separations* **2000,** *19* (2), 45-48.
(31) Ngamchuea, K.; Eloul, S.; Tschulik, K.; Compton, R. G. Planar diffusion to macro disc electrodes—what electrode size is required for the Cottrell and Randles-Sevcik equations to apply quantitatively? *J. Solid State Electrochem.* **2014,** *18* (12), 3251-3257.
(32) Miao, R.; Shao, L.; Compton, R. G. Single entity electrochemistry and the electron transfer kinetics of hydrazine oxidation. *Nano Research*. In press.
(33) Daniele, S.; Lavagnini, I.; Baldo, M. A.; Magno, F. Steady state voltammetry at microelectrodes for the hydrogen evolution from strong and weak acids under pseudo-first and second order kinetic conditions. *J. Electroanal. Chem.* **1996,** *404* (1), 105-111.
(34) Jiao, X.; Batchelor-McAuley, C.; Kätelhön, E.; Ellison, J.; Tschulik, K.; Compton, R. G. The subtleties of the reversible hydrogen evolution reaction arising from the nonunity stoichiometry. *The Journal of Physical Chemistry C* **2015,** *119* (17), 9402-9410.
(35) Laborda, E.; Henstridge, M. C.; Molina, A.; Martínez-Ortiz, F.; Compton, R. G. A comparison of Marcus–Hush vs. Butler–Volmer electrode kinetics using potential pulse voltammetric techniques. *J. Electroanal. Chem.* **2011,** *660* (1), 169-177.
(36) Ojha, K.; Farber, E. M.; Burshtein, T. Y.; Eisenberg, D. A Multi-Doped Electrocatalyst for Efficient Hydrazine Oxidation. *Angew. Chem. Int. Ed.* **2018,** *57* (52), 17168-17172.
(37) Wang, T.; Wang, Q.; Wang, Y.; Da, Y.; Zhou, W.; Shao, Y.; Li, D.; Zhan, S.; Yuan, J.; Wang, H. Atomically Dispersed Semimetallic Selenium on Porous Carbon Membrane as an Electrode for Hydrazine Fuel Cells. *Angew. Chem.* **2019,** *131* (38), 13600-13605.